Yang et al., Aerosol and Air Quality Research, Vol. 9, No. 2, pp. 266-276, 2009

A CE/SE Scheme for Flows in Porous Media and Its Applications

Duo-Xing Yang[1,2], Guo-Min Li[2*], De-Liang Zhang[3]

[1] *Institute of Crustal Dynamics, Chinese Earthquake Administration, Beijing 100085*
[2] *Institute of Geology and Geophysics, Chinese Academy of Sciences, Beijing 100029*
[3] *Institute of Mechanics, Chinese Academy of Sciences, Beijing 100080*

Abstract

In this paper, a new computational scheme for solving flows in porous media was proposed. The scheme was based on an improved CE/SE method (the space-time Conservation Element and Solution Element method).We described porous flows by adopting DFB (Brinkman-Forchheimer extended Darcy) equation. The comparison between our computational results and Ghia's confirmed the high accuracy, resolution, and efficiency of our CE/SE scheme. The proposed first-order CE/SE scheme is a new reliable way for numerical simulations of flows in porous media. After investigation of effects of Darcy number on porous flow, it shows that Darcy number has dominant influence on porous flow for the Reynolds number and porosity considered.

Key words: CE/SE; Porous media; Darcy law.

INTRODUCTION

Models for flow in porous media have been developed since 1856, when Darcy postulated his well-known equation. Vafai *et al.* (1980) pointed out the limitations of Darcy's law. For porous media with high permeability, both the viscous effects (frictional drag at the boundary) and the inertia (form-drag) effects within the porous matrix are significant. Consequently for Newtonian fluids, the non-Darcy effects of form-drag and boundary resistance have been studied extensively through the use of the Brinkman-Forchheimer extended Darcy model (DFB). One of the first papers to deal with these extensions was Vafai (1984). In recent years, the flow in porous media formulated by the DFB model was successfully used in a wide variety of flow conditions, including forced convection pipe flow (Alkman *et al.*, 1998), natural convection in vertically layered porous media (Hadim, 2006), and double-diffusive natural convection (Wang *et al.*, 2008). Numerical simulations for non-Darcy flows have improved immensely as a result of major progress in

* Corresponding author. Tel.: +86-10-82998620;
Fax: +86-10-82998620
E-mail address: guominli@mail.iggcas.ac.cn

both computational methods and available computer facilities.

Deiber and Bortolozzi (1998) applied vorticity-stream function scheme to study natural convection in a porous annulus. Rees (2002) analyzed the onset of Darcy-Brinkman convection in a porous layer by using an asymptotic analysis method. Sman (2002) numerically solved the DFB model with 3D finite element solver (FIDAP). Costa *et al.* (2004) used a two-dimensional laminar version of the control volume based finite element method to simulate non-Darcian flows through spaces partially filled with a porous media. Reis *et al.* (2004) applied the finite volume method to simulate the impact of liquid droplets on porous surfaces, using DFB model. However, this type of flow poses a major phenomenological and modeling challenge.

In this presentation, a CE/SE (space-time conservation element and solution element) scheme with first-order accuracy for porous flows is established by applying new structures of CEs (conservation element) and SEs (solution element) (Zhang *et al.*, 2001). The DFB model is used to represent the fluid transport within the porous medium. Governing partial differential equations are transformed to algebraic ones by CE/SE, and the pressure-velocity coupling problem is solved by using artifical pressure method over structured and staggered grids. We conduct DFB-based flow simulations for single phase flow through a 2D (two-dimensional) porous medium. A benchmarking problem is simulated numerically and computational results are carefully compared with that from other literature. Influences of Darcy numbers upon porous flows are investigated.

ANALYSIS AND MODELING

The continuity equation and the momentum equation for 2D incompressible and viscous flow in porous medium can be summarized as follows (Reis *et al.*, 2004).

Continuity:

$$\nabla^* \cdot \overline{U}^* = 0 \tag{1a}$$

Momentum balance of fluid:

$$\rho^* \frac{\partial \overline{U}^*}{\partial t^*} + \frac{\rho^*}{\phi}(\overline{U}^* \cdot \nabla^*)\overline{U}^* = -\phi \nabla^* P^* + \mu_e^* \nabla^{*2} \overline{U}^* - \frac{\phi \mu_f^*}{K}\overline{U}^* - \frac{\rho^* \phi F_b}{\sqrt{K}}\overline{U}^* \left|\overline{U}^*\right| + \rho^* g \phi \tag{1b}$$

where all constants and variables are defined in the nomenclature. Eq. (1a) and Eq. (1b) form the full set of equations used to model flows in porous media. Eq. (1b) contains the usual balance of forces between viscosity and pressure gradient known as Darcy's law (the 3rd and 5th terms), which is extended through the further inclusion of terms modeling in turn advective inertia (the 1st and 2nd terms), boundary effects (the 4th term: the Brinkman term) and form-drag (the 6th term: Forchheimer inertia). Quantities have been rendered dimensionless with respect to the characteristic length L, and the characteristic velocity u_o, using the definitions:

$$x = \frac{x^*}{L}, y = \frac{y^*}{L}, t = \frac{t^*}{\left(\frac{L}{u_o}\right)}, u = \frac{u^*}{u_o}, v = \frac{v^*}{u_o},$$

$$P = \frac{P^*}{\rho_o u_o^2}, \rho = \frac{\rho^*}{\rho_o}, \mu_f = \frac{\mu_f^*}{\mu_o}, \mu_e = \frac{\mu_e^*}{\mu_o},$$

$$Fr = \frac{u_o}{gL} \tag{2}$$

Eq. (1a) and Eq. (1b) take the forms

$$\nabla \cdot \overline{U} = 0 \tag{3a}$$

$$\frac{\partial \overline{U}}{\partial t} + \frac{1}{\phi}\overline{U}\nabla \cdot \overline{U} = -\frac{1}{\rho}\phi\nabla P + \frac{\alpha\mu_f}{\rho \,\mathrm{Re}}\nabla^2\overline{U} - \frac{\mu_f \phi}{\rho Da \,\mathrm{Re}}\overline{U} - \frac{\phi F_b}{\sqrt{Da}}\overline{U}\left|\overline{U}\right| + \frac{g\phi}{Fr} \tag{3b}$$

Where

$$Da = \frac{K}{L^2}, \mathrm{Re} = \frac{\rho_o L u_o}{\mu_o}, \alpha = \frac{\mu_e}{\mu_f} \tag{3c}$$

here $\overline{U} = (u, v)$, P , t , α and Da denote velocity vector, pressure, time , viscosity ratio and Darcy number, respectively. The nondimensional coefficients Re and F_b correspond to the Reynolds number and form-drag inertia term, respectively. Flow in porous media governed by Eq. (3b) is characterized by the porosity and three non-dimensional parameters: Reynolds number, Darcy number, and viscosity ratio.

The governing Eq. (3a) and Eq. (3b) can be rewritten as the Euler equation

$$\frac{\partial Q}{\partial t} + \frac{\partial E}{\partial x} + \frac{\partial F}{\partial y} = S \tag{4}$$

where Q , E , F , S are vectors of primary variable, flux in x-direction, flux in y-direction and source, respectively. This set of equations describes the conservation of density ρ , momenta $\rho\vec{v} = (\rho u, \rho v)$. The original two-dimensional CE/SE method (Chang *et al.*, 1999) is complicated as the special design of CEs and SEs. Zhang *et al.* (2001) proposed an improved CE/SE method by adopting general hexahedrons mesh to construct CEs and SEs, as shown in Fig. 1(b) and Fig. 1(c). The structure of CEs and SEs simplifies the process of scheme derivation. In this study, we deduce the two-dimensional CE/SE scheme with first-order accuracy for flows in porous medium. Let (j, k, n) denote a set of space-time mesh points, where $n = 0, \pm\frac{1}{2}, \pm 1, \pm\frac{3}{2}\ldots$ for time, $j = 0, \pm\frac{1}{2}, \pm 1, \pm\frac{3}{2}\ldots$ for x, $k = 0, \pm\frac{1}{2}, \pm 1, \pm\frac{3}{2}\ldots$ for y. A SE is defined as the vicinity of a mesh point and the whole space-time region is divided into non-overlapping CEs. Assume that the physical variables in every SE are approximated by the Taylor's expansions at the mesh point associated with the SE, and the conservation Eq. (4) is satisfied in every CE. Let $x_1 = x$, $x_2 = y$, $x_3 = t$ be considered as the coordinates of a Euclidean space E_3 . By means of the Gauss' divergence theorem, Eq. (4) is rewritten in form of

$$\oint_{\Omega(V)} H \cdot dS = \int_V S \cdot dV \tag{5}$$

where $H=(Q,E,F)$, $\Omega(V)$ is the boundary of an arbitrary space-time region V, $ds=d\sigma\cdot n$ with $d\sigma$ and n, respectively, being the area and the outward unit normal of a surface element on $\Omega(V)$. For any point $P'(t,x,y)$ of the solution element SE(P′), Q, E and F are approximated by Q^*, E^* and F^*, which are the first-order Taylor expansions of Q, E and F. Let

$$M^*(\delta x,\delta y,\delta t)_{P'}=M_{P'}+(M_x)_{P'}\delta x+(M_y)_{P'}\delta y+(M_t)_{P'}\delta t \quad (6)$$

here $M=Q,E,F$, and $\delta x=x-x_{P'}$, $\delta y=y-y_{P'}$, $\delta t=t-t_{P'}$. Substituting Eq. (6) into Eq. (4), we obtain

$$(Q_t)_{P'}=-(E_x)_{P'}-(F_y)_{P'}+(S)_{P'} \quad (7)$$

Eq. (6) and Eq. (7) imply that the variables required in computation are Q_x and Q_y. Integrating Eq. (5) on the surfaces of CE(P') and applying source item linearization method (Wang *et al.*, 2008), we obtain

$$(Q_m)_{P'}=\frac{1}{4}(\overline{Q}+\frac{\Delta t}{\Delta x}\overline{E}+\frac{\Delta t}{\Delta y}\overline{F})+\frac{\Delta t}{8}\widetilde{S} \quad (8)$$

$$\widetilde{S}=\overline{S}+\frac{\Delta t}{4}\overline{S}_t$$

Where

$$\overline{Q}=Q_m(A,\frac{\Delta x}{4},\frac{\Delta y}{4},0)+Q_m(C,-\frac{\Delta x}{4},\frac{\Delta y}{4},0)+Q_m(E,-\frac{\Delta x}{4},-\frac{\Delta y}{4},0)+Q_m(G,-\frac{\Delta x}{4},\frac{\Delta y}{4},0)$$

$$\overline{E}=E_m(A,0,\frac{\Delta y}{4},\frac{\Delta t}{4})-E_m(C,0,\frac{\Delta y}{4},\frac{\Delta t}{4})-E_m(E,0,-\frac{\Delta y}{4},\frac{\Delta t}{4})+E_m(G,0,-\frac{\Delta y}{4},\frac{\Delta t}{4}))$$

$$\overline{F}=F_m(A,\frac{\Delta x}{4},0,\frac{\Delta t}{4})+F_m(C,-\frac{\Delta x}{4},0,\frac{\Delta t}{4})-F_m(E,-\frac{\Delta x}{4},0,\frac{\Delta t}{4})-F_m(G,\frac{\Delta x}{4},0,\frac{\Delta t}{4})$$

$$\overline{S}=S_m(A)+S_m(C)+S_m(E)+S_m(G) \quad (9)$$

$\overline{S}_t$ is the time derivative of $\overline{S}$. Using the continuity conditions at points A', C', E' and G', the derivatives of Q with respect to x and y are obtained

$$(Q_x)_{P'}=W[(Q_x)^-_{P'},(Q_x)^+_{P'},\alpha]$$
$$(Q_y)_{P'}=W[(Q_y)^-_{P'},(Q_y)^+_{P'},\alpha]$$

here $(Q_x)^{\pm}_{P'}$, $(Q_y)^{\pm}_{P'}$ are defined as the following.

$$(Q_{mx})^-_{P'}=-\frac{1}{\Delta x}\left[Q_m(A,0,0,\frac{\Delta t}{2})+Q_m(G,0,0,\frac{\Delta t}{2})-2(Q_m)_{P'}\right]$$
$$(Q_{mx})^+_{P'}=+\frac{1}{\Delta x}\left[Q_m(C,0,0,\frac{\Delta t}{2})+Q_m(E,0,0,\frac{\Delta t}{2})-2(Q_m)_{P'}\right]$$
$$(Q_{my})^-_{P'}=-\frac{1}{\Delta y}\left[Q_m(A,0,0,\frac{\Delta t}{2})+Q_m(C,0,0,\frac{\Delta t}{2})-2(Q_m)_{P'}\right]$$
$$(Q_{my})^+_{P'}=+\frac{1}{\Delta y}\left[Q_m(E,0,0,\frac{\Delta t}{2})+Q_m(G,0,0,\frac{\Delta t}{2})-2(Q_m)_{P'}\right] \quad (10)$$

The weighted equation is $W[x_+,x_-,\alpha]=\frac{|x_+|^\alpha x_-+|x_-|^\alpha x_+}{|x_-|^\alpha+|x_-|^\alpha}$, and α is a constant (α = 2 in this study) (Chang 1995; Chang *et al.*, 1999).

The coupling between velocity and pressure is performed by artificial compressibility method (Chorin, 1967). Eq. (1a) can be rewritten in form of

$$\phi\frac{\partial P}{\partial \tau}+C^2\rho(\frac{\partial u}{\partial x}+\frac{\partial v}{\partial y})=0 \tag{11}$$

where τ is the visual time, and C^2 is the coefficient effecting the numerical stability. Substituting the visual time derivative of velocities into Eq. (1b), we obtain

$$\frac{\partial U}{\partial \tau}+\frac{\partial Q}{\partial t}+\frac{\partial E(Q)}{\partial x}+\frac{\partial F(Q)}{\partial y}=S(Q) \tag{12}$$

here $U=\begin{bmatrix}\frac{\phi}{C^2}P\\ u\\ v\end{bmatrix}$, for $\tau\to\infty$, Eq. (12) is consistent to Eq. (1b). Applying the pressure splitting method, Eq. (12) takes the form

$$\frac{\partial U_v}{\partial \tau}+\frac{\partial Q_v}{\partial t}+R_v(Q_v)+\frac{\phi}{\rho}\nabla P=0 \tag{13}$$

where

$$R_v(Q_v)=(\frac{\partial E_v(Q_v)}{\partial x}+\frac{\partial F_v(Q_v)}{\partial y}-S_v(Q_v)),$$

$$Q_v=U_v=\begin{bmatrix}u\\ v\end{bmatrix},\quad E_v=\begin{bmatrix}\frac{1}{\phi}u^2-\frac{\tau_{xx}}{\rho\,\mathrm{Re}}\\ \frac{1}{\phi}uv-\frac{\tau_{yx}}{\rho\,\mathrm{Re}}\end{bmatrix},$$

$$F_v=\begin{bmatrix}\frac{1}{\phi}uv-\frac{\tau_{xy}}{\rho\,\mathrm{Re}}\\ \frac{1}{\phi}v^2-\frac{\tau_{yy}}{\rho\,\mathrm{Re}}\end{bmatrix},$$

$$S_v=\begin{bmatrix}-\frac{\phi}{\rho Da\,\mathrm{Re}}u-\frac{\phi F_b}{\sqrt{Da}}u\sqrt{u^2+v^2}+\phi\frac{g_x}{Fr}\\ -\frac{\phi}{\rho Da\,\mathrm{Re}}v-\frac{\phi F_b}{\sqrt{Da}}v\sqrt{u^2+v^2}+\phi\frac{g_y}{Fr}\end{bmatrix}.$$

Using the time operator splitting method (Jue, 2000) to split pressure item in momentum Eq. (13), we obtain

$$\frac{Q_v^{n+\frac{1}{2}}-f(Q_v^n)}{\Delta t}+R_v^n(Q_v^n)=0 \tag{14a}$$

$$\frac{\partial U}{\partial \tau}+\frac{Q_v^{n+1}-Q_v^{n+\frac{1}{2}}}{\Delta t}+\frac{\phi}{\rho}\nabla P=0 \tag{14b}$$

We interpret Eq. (14a) as yielding an intermediate value of Q_v^n, denoted by $Q_v^{n+\frac{1}{2}}$ at time n. Here, the superscript n indicates the time step. $F(Q_v^n)$ is the value of Q_v^n at time step n. Eq. (14a) can be simulated by CE/SE method to obtain $Q_v^{n+\frac{1}{2}}$. By means of time-marching solutions and internal iteration method, Eq. (11) and Eq. (14b) yield

$$\phi\frac{P^{m+1}-f(P^m)}{\Delta\tau}+C^2(\frac{\partial u}{\partial x}+\frac{\partial v}{\partial y})^m=0 \tag{15a}$$

$$\frac{U^{m+1}-U^m}{\Delta\tau}+\frac{Q^{m+1}-Q^{n+\frac{1}{2}}}{\Delta t}+\frac{\phi}{\rho}\nabla P^{m+1}=0 \tag{15b}$$

where m is the iteration step. Assume that we have already carried out m iteration. Then, for the $m+1$ iteration, by substituting $Q_v^{n+\frac{1}{2}}$ into

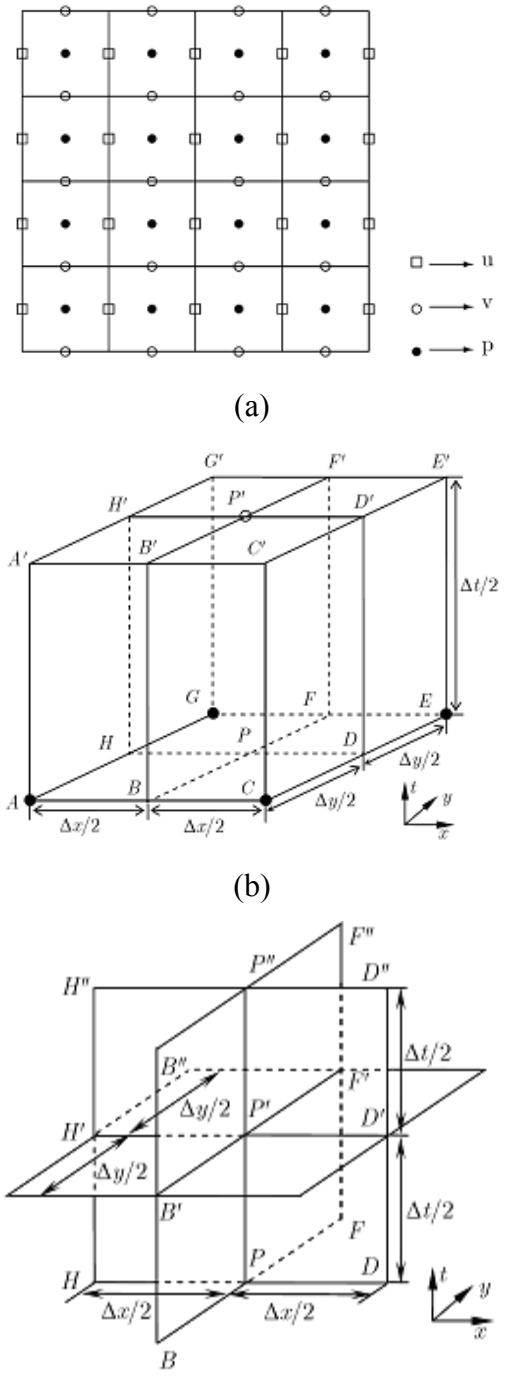

Fig. 1. Mesh construction of the improved CE/SE method. (a) Mesh points projection on *xy* plane, (b) Conservation element CE(P′), (c) Solution element SE(P′) .

Eq. (15a) and using CE/SE method, P^{m+1} can be calculated at iteration step $m+1$. Substituting P^{m+1} into Eq. (15b), U^{m+1} is obtained. The above procedure is repeated for a number of iteration, convergence is achieved when $U^{m+1}-U^{m}$ become less than a prescribed value (10^{-6}) at all grid points. After convergence, U^{n+1} can be obtained at time step $n+1$. These governing equations are discretized on staggered orthogonal grid (as shown in Fig. 1(a) which eliminates the possibility of a checkerboard pressure pattern.

NUMERICAL VALIDATION AND DISCUSSION

Numerical Validation

Here, we focus on the 2D square, lid-driven cavity filled with fluid-saturated porous medium. The driven cavity is a well-known benchmark problem for numerical methods for laminar flows due to the simple geometry and complicated flow behaviors. We apply the improved CE/SE method to the fluid flow in a square cavity filled with a porous medium. The flow condition is the same as that of lid-driven flow problem (Guo *et al.*, 2002) as shown in Fig. 2(a). At the left, right and down boundaries, no-slip condition holds at the wall, respectively. While, at the upper boundary, the horizontal velocity is specified and held fixed. Hence, in Fig. 2(a), $u=1.0$. The computational domain covered 202 × 202 grid used for the calculations. We set $Da = 10^4$, ϕ = 0.9 and Re = 100 and 1000. In Fig. 2 and Fig. 3, the velocity profiles through the cavity center are plotted. The benchmark solutions (Ghia *et al.*, 1982) are also included for comparison. It is seen that the CE/SE solutions

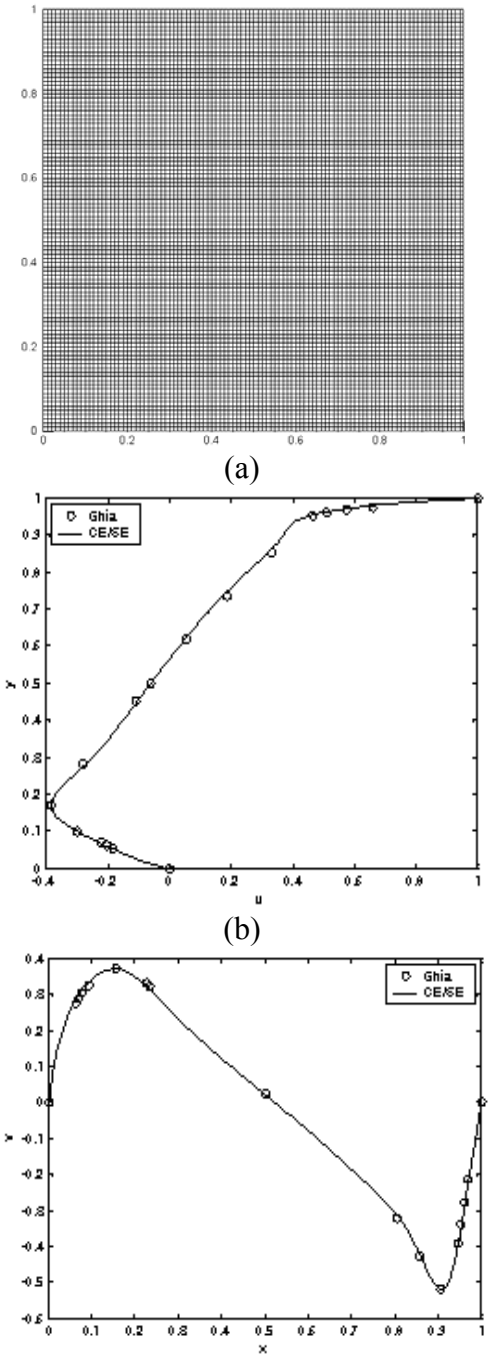

(a)

(b)

(c)

Fig. 2. Velocity profiles through the cavity center. Solid lines are CE/SE solutions, and symbols are benchmark solutions by Ghia. (a) Grid schematic for the boundary conditions, (b) u component along the vertical line through the cavity center, (c) v component along the horizontal line through the cavity center (ϕ = 0.9, $Da = 10^4$, Re = 1000).

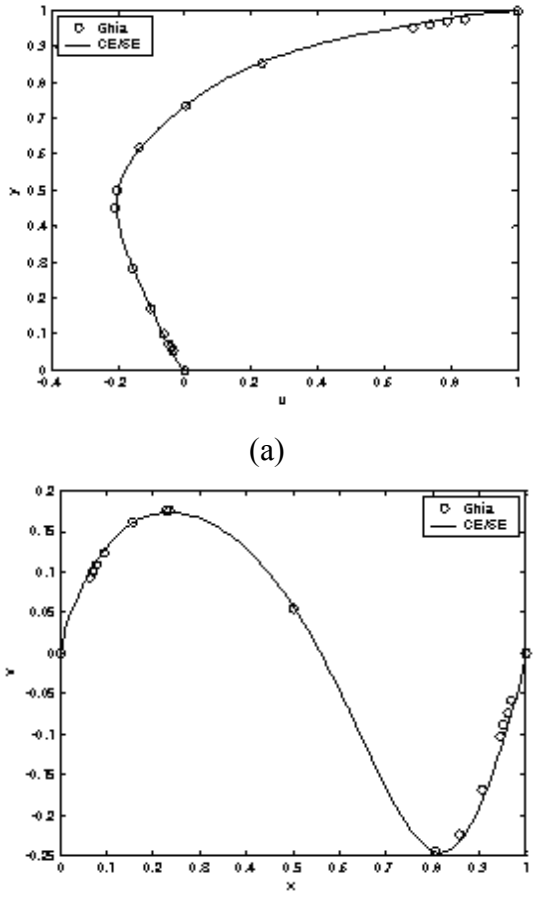

(a)

(b)

Fig. 3. Velocity profiles through the cavity center. Solid lines are CE/SE solutions, and symbols are benchmark solutions by Ghia. (a) u component along the vertical line through the cavity center, (b) v component along the horizontal line through the cavity center (ϕ = 0.9, $Da = 10^4$, Re = 100).

agree well with the benchmark solutions for the cases considered. Fig. 4 shows the eddies of the cavity for Re = 1000 and 100, respectively. As expected, the vortex has somewhat strengthened with the increase in Reynolds number. It is inferred that the effects of Darcy's law and form-drag in the DFB model on the porous flows are neglectable for $Da = 10^4$ and $\phi = 0.9$ considered.

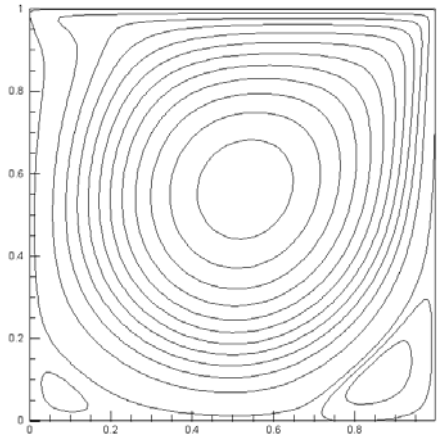

(a)

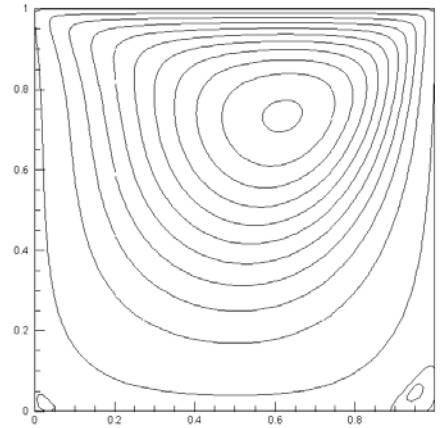

(b)

Fig. 4. Stream lines for $\phi = 0.9$, $Da = 10^4$ at (a) Re = 1000, (b) Re = 100.

Discussion

In this case, study is carried out for $\phi = 0.1$ and Re = 10 and $Da = 10^{-1}$, 10^{-2}, 10^{-3} and 10^{-4}. Variation of u and v-velocity for $Da = 10^{-1}$, 10^{-2}, 10^{-3} and 10^{-4} is shown in Fig. 5. It can be observed that by the reduction of Darcy number from 10^{-1}, the velocities get reduced due to the obstruction for the flow, which resulted from the solid matrix. As shown in Fig. 5(b), by the reduction of Darcy number from 10^{-1} to 10^{-4} the boundary layer near the moving lid becomes thinner and the vortex becomes weaker and tends to move up, towards the lid. The effect of Darcy number for $\phi = 0.1$ and Re = 10 is shown in Fig. 6. Considering a Darcy number of 10^{-1}, it is noted that formation of two secondary vortices takes place at the left bottom and right bottom corners. These vortices slowly diminish and vanish with further reduction of Darcy number. It's proved that the lid-driven cavity flow in porous medium is significantly influenced by Darcy number for the Reynolds number and porosity considered.

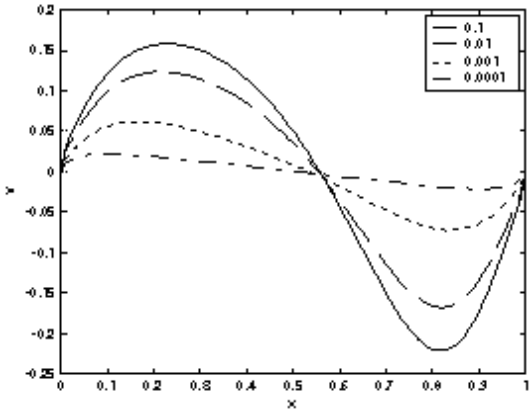

(a)

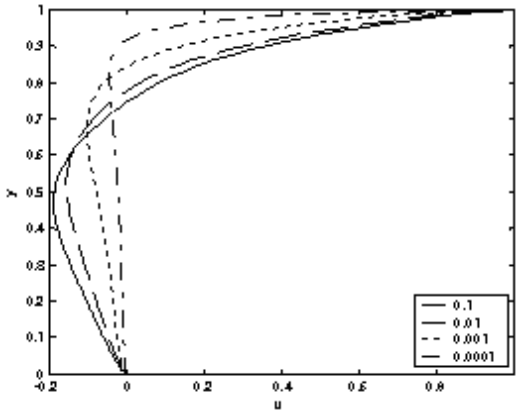

(b)

Fig. 5. Velocity profiles through the cavity center for different Darcy number ($Da = 10^{-1}$, 10^{-2}, 10^{-3} and 10^{-4}). (a) v component along the vertical line through the cavity center, (b) u component along the horizontal line through the cavity center ($\phi = 0.1$, Re = 10).

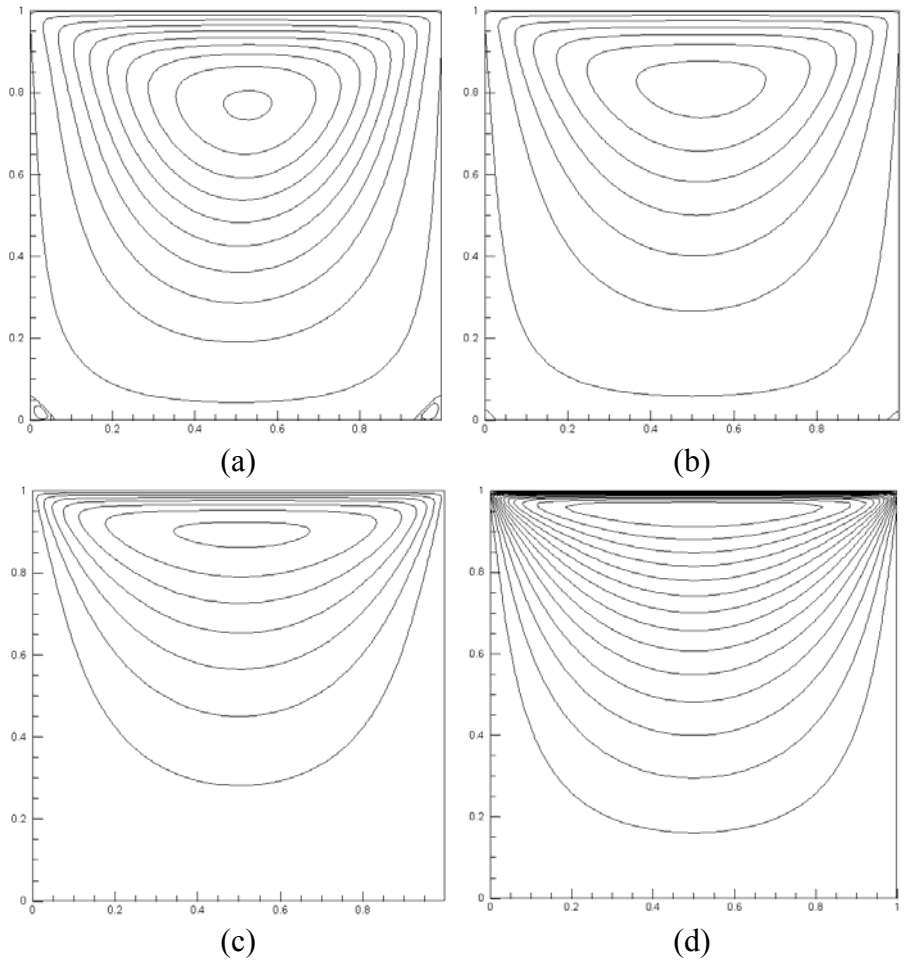

Fig. 6. Stream lines for $\phi = 0.1$, Re = 10: (a) $Da = 10^{-1}$, (b) $Da = 10^{-2}$, (c) $Da = 10^{-3}$, (d) $Da = 10^{-4}$.

SUMMARY

An improved two-dimensional CE/SE scheme has been extended to DFB model to simulate flows in porous medium. The accuracy of the new CE/SE scheme is validated by comparing the numerical results of lid-driven cavity flow with the corresponding results by Ghia *et al.* (1982) It is observed for the Reynolds number and porosity considered, as the Darcy number is reduced the primary vortex becomes weaker and tends to move towards the lid. Secondary vortices formed at higher Darcy numbers (10^{-1} and 10^{-2}) diminish and lead to single vortex near to the lid by the reduction of Darcy number. The proposed first-order CE/SE scheme is a new reliable way for numerical simulation of flows in porous medium. Further work will be required to improve CE/SE computational efficiency by using multi-grid method.

ACKNOWLEDGMENTS

This work was supported by Institute of Crustal Dynamics (ZDJ2008-08) and National "973 Project" of China (2006CB705802). The

authors also greatly appreciate Prof. Chuen-Jinn Tsai, as well as the anonymous reviewers for their constructive comments, which have much improved this manuscript.

REFERENCES

Alkman, M.K. and Alnimr, M.A. (1998). Transient Non-Darcian Forced Convection Flow in a Pipe Partially Filled with a Porous Material. *Int. J. Heat Mass Transfer* . 41: 347-356.

Allan, F.M. and Hamdan, M.H. (2002). Fluid Mechanics of the Interface Region between Two Porous Layers. *Appl. Math. Comput.* 128: 37-43.

Chang, S.C. (1995). The Method of Space-Time Conservation Element and Solution Element–A New Approach for Solving the Navier-Stokes and Euler Equations. *J. Comput. Phys.* 119: 295-324.

Chang, S.C., Wang, X.Y., and Chow CY. (1999). The Space-Time Conservation Element and Solution Element Method: A New High-resolution and Genuinely Multidimensional Paradigm for Solving Conservation Laws. *J. Comput. Phys.* 156: 89-136.

Chorin, A.J. (1967). A Numerical Method for Solving Incompressible Viscous Flow Problem. *J. Comput. Phys.* 2: 12-26.

Costa, V.A.F., Oliveira, M.S.A. and Sousa, A.C.M. (2004). Numerical Simulation of Non-Darcian Flows Through Spaces Partially Filled with a Porous Media. *Comput. Struct.* 82: 1535-1541.

Deiber, J.A. and Bortolozzi, R.A. (1998). A Two-Field Model for Natural Convection in a Porous Annulus at High Rayleigh Numbers. *Chem. Eng. Sci.* 53: 1505-1516.

Ghia, U., Ghia, K.N. and Shin, C.T. (1982). High-Re Solutions for Incompressible Flow Using the Navier-Stokes Equations and a Multigrid Method. *J. Comput. Phys.* 48: 387-411.

Guo, Z.L. and Zhao, T.S. (2002). Lattice Boltzmann Model for Incompressible Flows Through Porous Media. *Phys. Rev. E.* 66: 036304.

Hadim, H. (2006). Non-Darcy Natural Convection of a Non-Newtonian Fluid in a Porous Cavity. *Int. Commun. Heat Mass Transfe.* 33: 1179-1189.

Jue, T.C. (2000). Analysis of Oscillatory Flow with Thermal Convection in a Rectangular Cavity Filled with Porous Medium. *Int. Commun. Heat Mass Transfer.* 27: 985-994.

Rees, D.A.S. (2002). The Onset of Darcy-Brinkman Convection in a Porous Layer: An Asymptotic Analysis. *Int. Commun. Heat Mass Transfer.* 45: 2213-2220.

Reis, Jr. N.C., Griffiths, R.F. and Santos, J.M. (2004). Numerical simulation of the Impact of liquid Droplets on Porous Surfaces. *J. Comput. Phys.* 198: 747-770.

Sman, R.G.M. (2002). Prediction of Airflow through a Vented Box by the Darcy-Forchheimer Equation. *J. Food Eng.* 55: 49-57.

Vafai, K. and Tien, C. (1980). Boundary and Inertial Effects of Convective Mass Transfer in Porous Media. *Int. J. Heat Mass Transfer.* 25: 1183-1190.

Vafai, K. (1984). Convection Flow and Heat

Transfer in Variable Porous Media. *J. Fluid Mech.* 147: 233-259.

Wang, J. Liu, K.X. and Zhang, D.L. (2008). An Improved CE/SE Scheme for Multi-Meterial Elastic-Plastic Flows and Its Application. *Comput. Fluids.* 38: 544-551.

Wang, S. and Tan, W.C. (2008). Stability Analysis of Double-Diffusive Convection of Maxwell Fluid in a Porous Media Heated from below. *Phys. Lett. A.* 372: 3046-3050.

Zhang, D.L., Xie, W., Guo, C.M. and Hu, X.Y. (2001). Numerical Simulation of Cellar Structures and Mach Reflection of Gaseous Detonation Waves. *Explo. Shock Wave.* 21: 161-167.

Received for review, January 4, 2009
Accepted, March 9, 2009